

Compartmentalization of an all-*E. coli* Cell-Free Expression System for the Construction of a Minimal Cell

Filippo Caschera^{*,**,*†}
Vincent Noireaux^{*,**}
University of Minnesota

Keywords

Cell-free transcription–translation, synthetic biology, minimal cell, encapsulation, gene circuits, cell-free metabolism

Abstract Cell-free expression is a technology used to synthesize minimal biological cells from natural molecular components. We have developed a versatile and powerful all-*E. coli* cell-free transcription–translation system energized by a robust metabolism, with the far objective of constructing a synthetic cell capable of self-reproduction. Inorganic phosphate (iP), a byproduct of protein synthesis, is recycled through polysugar catabolism to regenerate ATP (adenosine triphosphate) and thus supports long-lived and highly efficient protein synthesis *in vitro*. This cell-free TX-TL system is encapsulated into cell-sized unilamellar liposomes to express synthetic DNA programs. In this work, we study the compartmentalization of cell-free TX-TL reactions, one of the aspects of minimal cell module integration. We analyze the signals of various liposome populations by fluorescence microscopy for one and for two reporter genes, and for an inducible genetic circuit. We show that small nutrient molecules and proteins are encapsulated uniformly in the liposomes with small fluctuations. However, cell-free expression displays large fluctuations in signals among the same population, which are due to heterogeneous encapsulation of the DNA template. Consequently, the correlations of gene expression with the compartment dimension are difficult to predict accurately. Larger vesicles can have either low or high protein yields.

I Introduction

Biochemical systems with increasing complexity are now constructed outside living organisms using reductive bottom-up approaches [2, 18, 26, 27]. One experimental path to constructing minimal cells from scratch, arguably one of the most challenging cell-free projects, is to integrate and link three modules: self-organization (container), metabolism, and information [5, 35]. The integration of cellular parts into cell-sized liposomes aims at generating an out-of-equilibrium system that, ultimately,

Author Contributions: F.C. performed the experiments; F.C. and V.N. analyzed the data and wrote the manuscript.

* Contact author.

** Department of Physics, University of Minnesota, Minneapolis 55455, Minnesota. E-mail: filippocaschera@gmail.com (F.C.); noireaux@umn.edu (V.N.)

† Current address: Department of Chemical and Biochemical Engineering, Northwestern University, Evanston 60208, Illinois.

will be capable of self-maintenance and self-reproduction [23]. Cell-free transcription–translation (TX-TL) systems, from *E. coli* in particular, are becoming prominent platforms to assemble minimal cells using this approach [23]. The system is composed of a cytoplasmic extract that provides the TX-TL molecular machinery to execute DNA programs, and of a custom-made reaction solution to energize TX-TL, highly demanding in chemical energy [4, 7, 30]. The important feature of cell-free expression systems is their barrier-free environment. This allows precise concentration settings of the biochemical components involved in complex biological networks, either gene circuits or metabolic pathways [5, 13, 30]. Compartmentalization and compartment dynamics are necessary to create a genotype–phenotype linkage and guarantee evolvability of synthetic minimal cells [8, 39]. Evolution of an artificial cell goes beyond the concept of compartmentalized directed evolution [16]. A minimal cell is a complex system, constructed in laboratory through a hierarchical assembly of parts and modules that, at the end, has to show autonomy and open-ended evolution [5, 28].

The synthetic DNA program (genes and regulation) expressed inside liposomes will ultimately control most of the minimal cell functionalities. For instance, it will direct the synthesis of membrane proteins for nutrient exchange between the inner and outer solutions and the synthesis of phospholipids for volume expansion [5, 17, 21, 24]. Ribosome synthesis will be also encoded in synthetic DNA [14], as well as division directed by cytoskeletal proteins [20]. However, a DNA program is not enough. Biochemical and biophysical properties are also essential to achieve these complex functions, in particular self-assembly. Molecular crowding, for instance, is an essential condition to achieve and accelerate self-organization processes, from simple protein oligomerization to supramolecular assemblies of active cytoskeletal structures [41, 34]. Results for each of the minimal cell modules have been described, but integration into a functional unit has not been achieved [5].

One of the bottlenecks in such projects is the vast space of biochemical parameters. In the laboratory, the design of a minimal cell relies on the optimization of the interactions of many biochemical variables, some of which are coupled nonlinearly. To tackle this combinatorial problem we envision that high-throughput screening performed by liquid-handling robots will accelerate the navigation through the parameter space to provide necessary optimization at all the levels (cell-free TX-TL efficiency, gene circuits, metabolism scheme, etc.). The robotic workstations will be driven by predictive algorithms, which are based on statistical modeling of the fitness landscape [9, 11, 33]. Evolutionary robotics and virtual experiments [1] may help to define an optimal configuration of the robot hardware, which will be adapted for the synthesis of a minimal cell in laboratory [10, 12, 32].

Another bottleneck of minimal cell synthesis is the encapsulation of complex cell-free TX-TL reactions into liposomes. While many methods are available to prepare phospholipid vesicles, the reproducible formation of unilamellar liposomes at high concentrations of macromolecules and salts (physiological conditions) is a nontrivial problem [40].

In this article, we present an all-*E. coli* cell-free TX-TL energized by a powerful metabolic pathway based on the catabolism of di- and polysaccharides (maltose and maltodextrin) for the regeneration of ATP and recycling of inorganic phosphate [7], an inhibitory byproduct of protein synthesis. We present quantitative fluorescence measurements of the encapsulation of discrete molecular components (nucleosides, proteins, and DNA). We characterize protein synthesis of one reporter gene, of two reporter genes on two different plasmids, and of an inducible gene circuit. We show that the large fluctuations observed in signals are due to the encapsulation of large macromolecules (DNA), which is heterogeneous at low concentrations.

2 Materials and Methods

2.1 Cell-free Extract Preparation and In Vitro Protein Synthesis

The preparation and composition of the all-*E. coli* cell-free extract has been reported in our previous works [7, 37]. Cell-free reactions were performed as previously described, with either 12–15 mM maltose or 35 mM maltodextrin [7].

2.2 Plasmids

The plasmids used in this study are as follows: pBEST-OR2-OR1-Pr-UTR1-deGFP-T500, which was described previously [31], was used for cloning of the CFP and mCherry genes to create pBEST-OR2-OR1-Pr-UTR1-deCFP-T500 and pBEST-OR2-OR1-Pr-UTR1-mCherry-T500. The melibiose operon—including the melibiose repressor and its promoter (both denoted melR) and the regulatory parts upstream, melA-melB (Pmel)—was cloned into pBEST-OR2-OR1-Pr-UTR1-deGFP-T500 so as to remove the regulatory part OR2-OR1-Pr and make the plasmid pBEST-melR-Pmel-deGFP-T500 inducible with melibiose. All the plasmids were amplified, purified, and quantified as previously described [31].

2.3 Liposome Preparation

Liposomes were prepared using the emulsion transfer method [24, 15]. Solid POPC (1-palmitoyl-2-oleoyl-sn-glycero-3-phosphocholine, Avanti Polar Lipids Inc., USA) was dissolved at 10 mg/mL in liquid paraffin (Wako Chemicals, Inc., USA) and transferred into 1.5-ml tubes for dilution at 2 mg/mL. Afterward, lipids in paraffin were kept at 50°C for 50 min and stored in the dark for an hour before liposome generation. POPC in paraffin was transferred in a glass vial, and 2 μ L of inner solution (cell-free reaction) was added: 33% (v/v) S30 *E. coli* cellular extract, 60 mM K-glutamate, 5 mM Mg-glutamate, 1X 3-PGA buffer [7, 37], pBEST-OR2-OR1-Pr-UTR1-deGFP-T500 [31] at different concentrations depending on the experiment, 12 mM maltose or 35 mM maltodextrin, 2% PEG-8000 (v/v). Shaking the vial with a vortex at maximum speed for 5 s produced a water-in-oil emulsion. Then, 200 μ L of that emulsion were transferred onto 20 μ L of the outer feeding solution (1.5-ml tube), which contained the same components as the cell-free reactions except extract (replaced by S30B buffer), DNA (replaced by water), and BSA (replaced by water). The difference in osmotic pressure was balanced by addition of an excess of PEG-8000 in the feeding solution, 6% (v/v). The tube was centrifuged at 1500g for 10 min. After centrifugation the oil phase was removed and the liposome suspension was collected for microscope analysis. BSA-TRITC (Sigma-Aldrich), FITC-UTP (Invitrogen, USA) and DNA labeling kit (Mirus Bio LLC, USA) were used for liposome fluorescence. All of the other chemicals were purchased from Sigma-Aldrich (St. Louis, USA).

2.4 Microscope Image Analysis

After liposome generation, 10 μ L was dispensed on a microscope slide closed with a frame seal (Fisher Scientific, USA). Beads for the calibration line were purchased from SpheroTech, Inc., USA. The sealed microscope slides were incubated overnight at 29°C to carry out protein synthesis inside liposomes. Characterization of compartmentalized gene expression or molecular component encapsulation was performed with an inverted microscope IX81 (Olympus) equipped with a camera and proper sets of filters. A 40 \times air objective was used for observation. Image analysis was conducted with Olympus MetaMorph software. Fluorescence analysis was conducted using (1) CFP-2432A-OMF; filter Ex, 438/24 nm, Em: 483/32 nm, DM, 458; (2) GFP-3035D-OMF; filter Ex: 473/31 nm, Em: 520/35, nm DM: 495; and (3) TRITC filter ST, Ex: 525/4 nm, Em: 585/40 nm, DM: 555.

3 Results and Discussion

We first present results about improved in vitro protein synthesis obtained with our custom-made all-*E. coli* cell-free expression system [7]. In the second subsection the cell-free system is encapsulated into unilamellar liposomes. We characterize the encapsulation of various molecules making the cell-free reactions as a function of liposome size.

3.1 Enhanced Protein Synthesis with Glycolysis Intermediates

About 2 mg/mL of active reporter protein is synthesized in a batch mode reaction using an *E. coli* promoter specific to sigma factor 70 (primary sigma factor), with 3 mM amino acids. It corresponds

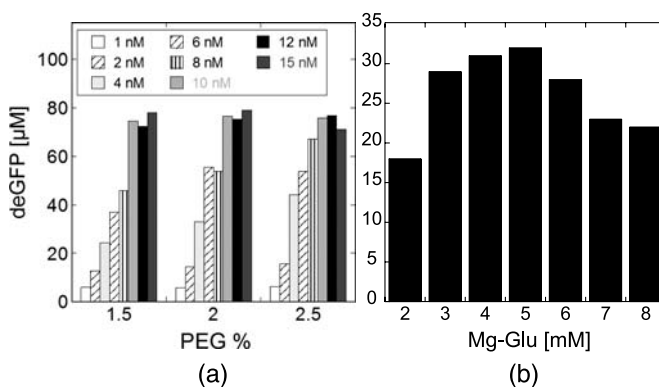


Figure 1. Cell-free protein synthesis in batch mode (12- μL reactions, 12 h at 29°C). (A) Cell-free synthesis of deGFP as a function of plasmid concentration (pBEST-OR2-OR1-Pr-UTR1-deGFP-T500) and amount of the molecular crowding agent (PEG-8000). (B) Optimization of transcriptional activation cascade (0.2 nM pBEST-OR2-OR1-Pr-UTR1-Sigma28-T500 and 5 nM pBEST-Ptar-UTR1-deGFP-T500) with magnesium glutamate.

to about 2.5 mg/ml of total protein synthesized (about 80% active). Settings of the various chemicals (about 15–20 without including the 20 amino acids) is done by hand to optimize expression. The concentration of deGFP, a modified version of eGFP described previously [31], is quantified against a calibration line built with known concentrations of a commercial green fluorescence protein [7]. The optimization consists of changing the plasmid concentration with different amount of molecular crowding agent (polyethylene glycol 8000, Figure 1A). PEG-8000 is added to the cell-free reaction to emulate the internal crowded cellular environment and thus accelerate molecular interaction kinetics. PEG-8000 is important to increase protein yields, and showed a concentration optimum between 1 and 2% (v/v). The largest achieved yield of active reporter protein is 80 μM deGFP (i.e., 2.0 mg/mL), and is obtained with a plasmid concentration between 10 and 15 nM. This result represents an improvement of 220% over the yield reported previously [30]. This increase was made possible by using a novel metabolic scheme that efficiently recycles iP through maltose or maltodextrin catabolism for sustained ATP production during *in vitro* protein synthesis [7]. This work contributes to the development of a robust metabolism module for minimal cells [6]. Our custom-made cell-free expression system recapitulates the entire sigma factor transcription scheme of *E. coli*. The six other *E. coli* sigma factors (sigma 19, 24, 28, 32, 38, 54) can be expressed to cascade on their respective promoters. Results for the sigma 28 cascade (pBEST-OR2-OR1-Pr-UTR1-UTR1-sigma28-T500 and pBEST-Ptar-UTR1-deGFP-T500) show also an increase of protein synthesis compared to our previous system [30] (Figure 1B). Magnesium is one of the most sensitive biochemicals for *in vitro* protein synthesis. About 30 μM of active deGFP is produced through the sigma 28 cascade with 1.5 mM of each of the 20 amino acids at a magnesium concentration of 4–5 mM.

3.2 Characterization of Component Encapsulation and Gene Expression in Liposome Populations

The encapsulation of cell-free reactions into phospholipids vesicles is a key step in the construction of minimal cells. Because cell-free TX-TL mixtures are extremely complex (high protein, salt, and nutrient concentrations) the production of unilamellar liposomes is highly dependent on the overall chemical composition and methodology used. After encapsulation, concentrations of the various components making a cell-free reaction are different from those in the initial mixture prepared in the test tube, as already observed for small liposomes [19]. In this work, we measured, after encapsulation, the concentration of three classes of molecules added to a cell-free reaction prepared with our all-*E. coli* TX-TL system: small ones (nutrients, using FITC-UTP \approx 0.5 nm, 1 kDa),

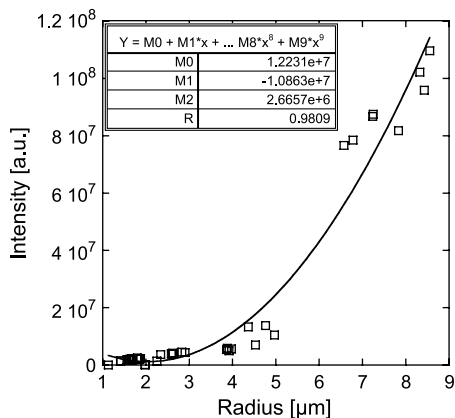


Figure 2. Image analysis of fluorescent polystyrene beads of different radius. Fluorescence intensity was measured through the GFP channel on an inverted microscope. Inset: fitting of the data points to a polynomial function.

medium-size ones (proteins, using BSA-TRITC \approx 5 nm, 60 kDa), and large ones (plasmid DNA 4 kbp labeled with TRITC \approx 250 nm as an ideal coil of Kuhn length 100 nm, 2500 kDa). We used fluorescence microscopy to measure the signal of population of spherical liposomes of diameter comprised between 2 and 20 μ m.

First, uniformly labeled fluorescent polystyrene beads of different diameters were used to build a standard curve as benchmark, characteristic of our optics (inverted microscope, 40 \times air objective with numerical aperture 0.6). The intensity versus bead size was fitted with a quadratic function (Figure 2) that reflects the geometry of the illuminated section of the spherical object (roughly a disk, and a depth of field of 1 μ m).

The encapsulation of the nucleoside triphosphate UTP labeled with fluorescein was measured as a probe for small nutrients below nanometer size (Figure 3A). To avoid signal saturation, the entrapment inside unilamellar vesicles was studied in the micromolar range (1, 5, and 10 μ M). As expected, the encapsulation depends on the liposome diameter and dye concentration (Figure 3B). At large diameter, the ratio of the fit of 5 μ M UTP fluorescein to that of 1 μ M is 6, and the ratio of the fit of 10 μ M UTP fluorescein to that of 1 μ M is 8. The entrapment of small nutrients corresponds fairly well to the concentration found in large test tube volumes and is fairly uniform, with good least squares. We performed the same experiment with the plasmid DNA template (Figure 3C). The plasmid was labeled covalently with TRITC (rhodamine), and then added to a cell-free reaction in the nanomolar range before encapsulation. We used the same procedure and method of analysis (Figure 3D). At concentrations of 1 and 5 nM plasmid, encapsulation slightly increased with the radius of the liposomes. At a concentration of 20 nM plasmid, however, the signal distribution can be fitted with a parabolic function with good least squares. This experiment shows how the process of encapsulation of large molecules changes nonlinearly, at low concentration, with respect to the concentration in test tubes.

Next, we studied the expression of the reporter protein deGFP inside phospholipids vesicles, using 5 nM plasmid (Figure 4A). The protein BSA labeled with TRITC (BSA-TRITC, 1.5 μ M final concentration) was also added to the cell-free reaction to study the encapsulation of proteins. The leak of fluorescence from one channel to the other was negligible. The gene expression was normalized and compared with the encapsulation of fluorescence BSA-TRITC protein. While the encapsulation of the protein can be fitted with a quadratic function with excellent least squares, the results for gene expression are much more scattered (Figure 4B). The encapsulation of large molecules (DNA template and possibly ribosomes) seems to be the origin of such heterogeneity of gene expression. The DNA template seems to be of greater importance for the fluctuations, because of its low concentration (1–50 nM) compared to that of ribosomes (1–2 μ M). For a liposome of 5- μ m

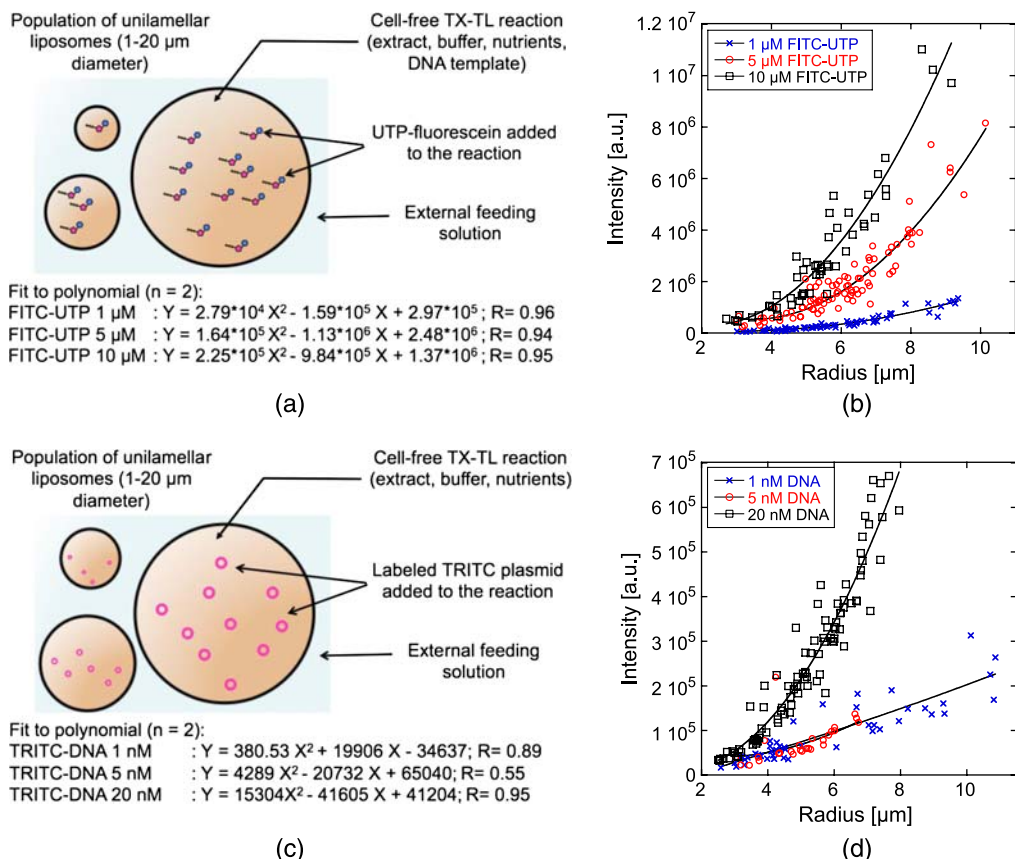


Figure 3. Microscope image analysis of unilamellar liposome populations. (A) Schematic of unilamellar liposomes with labeled UTP and polynomial fits. (B) Encapsulation of FITC-UTP at different concentrations (FITC-UTP was diluted in a cell-free reaction with no DNA). (C) Schematic of unilamellar liposomes with labeled DNA plasmid and polynomial fit. (D) Encapsulation of fluorescently labeled (TRITC) plasmid pBEST-OR2-ORI-Ptar-UTRI-deGFP-T500 at different concentrations (the plasmid was diluted in a cell-free reaction). Fluorescence intensity measured through TRITC channel. Data points are fitted with a quadratic function.

radius, the number of plasmids (5 nM) is on the order of 1600 (and at least 200 times more for ribosomes). Still, it is surprising to see such fluctuations at relatively large liposome sizes. Large fluctuations after encapsulation have been observed also for smaller liposomes [25, 36]. Gene expression was studied for three different plasmid concentrations (Figure 4C). Gene expression at 1 nM is low. At 5 nM plasmid gene expression is scattered, with large vesicles showing either low or high fluorescence (Figure 4D). However, with 25 nM plasmid, gene expression is more homogeneous. Gene expression inside liposomes was also studied for the two reporter proteins CFP and mCherry, cloned in two different plasmids encapsulated at the same time at 5 nM each (Figure 5A). Results were normalized to the vesicle showing the largest signal. As expected, gene expression is scattered for both colors (with a slight parabolic trend), and no correlation between the two signals could be made at the single liposome level (Figure 5B).

Finally, we constructed the melibiose regulatory system from *E. coli* into a single plasmid. This system is similar to the arabinose regulatory system. The melibiose repressor melR is expressed constitutively from its promoter. In the absence of melibiose in the medium, melR represses the transcription of the melA-B operon through a regulatory part that includes multiple operators. In the presence of melibiose, melR activates the transcription of melA-B. We clone deGFP under the

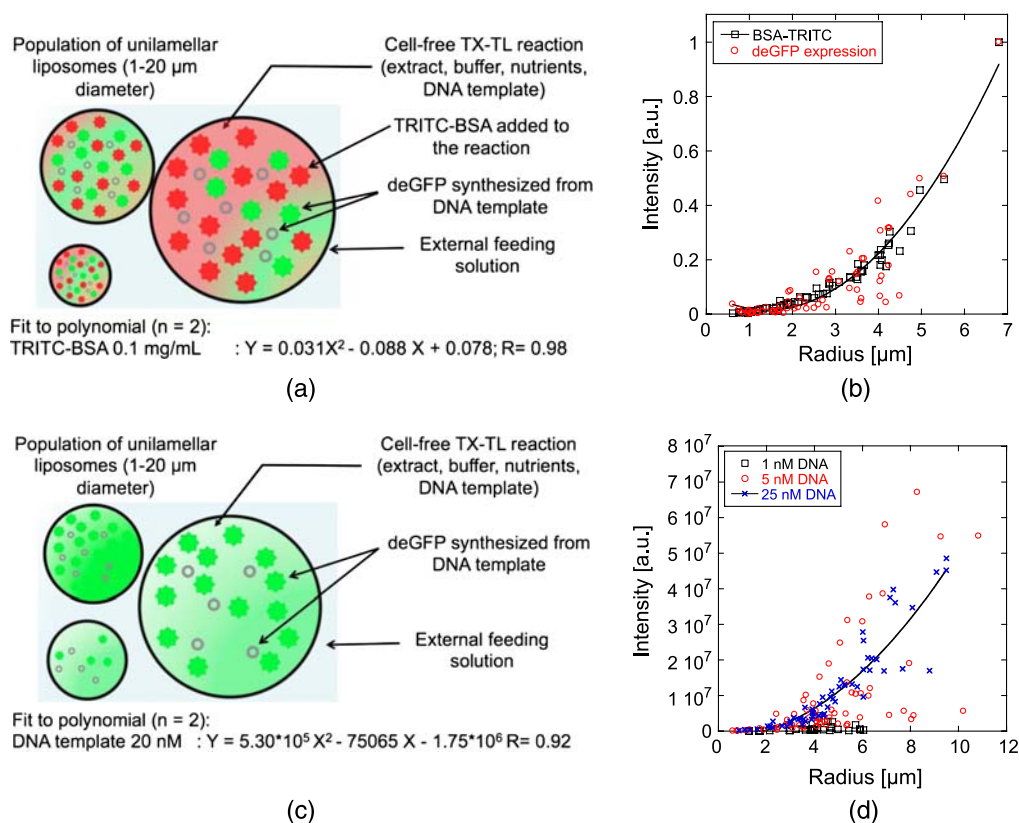


Figure 4. Microscope image analysis of unilamellar liposome populations. (A) Schematic of unilamellar liposomes expressing deGFP with labeled BSA and polynomial fit. (B) Co-encapsulation of BSA-TRITC at 0.1 mg/mL and plasmid pBEST-OR2-ORI-Pr-UTRI-deGFP-T500 (5 nM). Fluorescence intensity measured through TRITC and GFP channels after 12 h incubation at 29°C. The liposome radius reported was measured using the signal from FITC channel, and for comparison, data were normalized to the larger vesicle with higher intensity. Data points were fitted with a quadratic function. (C) Schematic of unilamellar liposomes expressing deGFP from different DNA concentration and polynomial fit. (D) Compartmentalized protein synthesis with different concentration of plasmid pBEST-OR2-ORI-Ptar-UTRI-deGFP-T500 after 12 h of incubation at 29°C. Fluorescence intensity measured through GFP channel. Data points are fitted with a quadratic function.

melibiose promoter operator. The genetic construct (10 nM) was encapsulated into vesicles (Figure 5C). Melibiose was added in three different ways: outside only, inside and outside, and neither inside nor outside. Without melibiose, the signal was at background level for any liposome radius (Figure 5D). Interestingly, no net difference was observed when melibiose was added either outside only or on both sides (in the feeding and in the liposomes). This indicates that melibiose could freely pass the phospholipid bilayer without any specific membrane channel. In both cases, however, expression was scattered with a slight parabolic trend.

4 Conclusions and Perspectives

In this work we made preliminary studies of the encapsulation into cell-sized liposomes of the most powerful all-*E. coli* cell-free TX-TL system so far reported. This cell-free toolbox is fueled with a novel metabolic scheme based on a carbon source for the regeneration of chemical energy

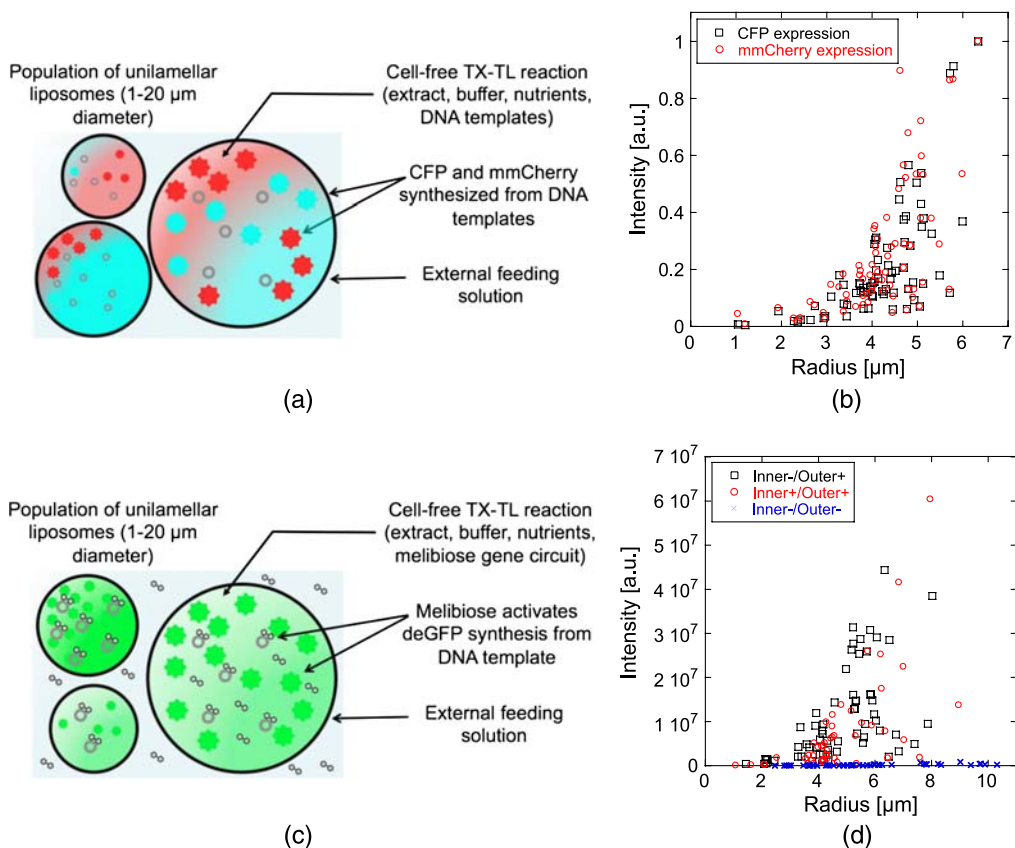


Figure 5. Microscope image analysis of unilamellar liposome populations. (A) Schematic of unilamellar liposomes expressing CFP and mCherry from DNA templates. (B) Co-encapsulation of 5 nM pBEST-OR2-OR1-Pr-UTR1-CFP-T500, 5 nM pBEST-OR2-OR1-Pr-UTR1-mCherry-T500, and compartmentalized protein synthesis. Fluorescence intensity measured through CFP and TRITC channel after 12 h of incubation at 29°C. The liposome radius reported was measured using the signal from the FITC channel, and for comparison, data were normalized to the larger vesicle with higher intensity. (C) Schematic of unilamellar liposomes encapsulating melibiose gene circuit and expressing deGFP. (D) Compartmentalized protein synthesis of the melibiose gene circuit (pBEST-melR-Pmel-deGFP-T500, 10 nM) with and without melibiose (10 mM), partitioned between inner and outer liposome solutions. Fluorescence intensity measured through GFP channel after 12 h of incubation at 29°C.

(ATP, GTP) and for the recycling of inorganic phosphate, a strong inhibitory byproduct of TX-TL reaction [6, 7].

Di- and polysaccharides (maltose and maltodextrin) can be used to activate glycolysis and produce ATP in turns, available for protein synthesis. Endogenous enzymes, which are already present in the cellular extract, are exploited to activate the central metabolism and sustain molecular machines' activity. Nucleoside triphosphates (ATP and GTP) are regenerated using catalysis also present in *E. coli*-based crude extract [3, 38]. Gene circuits are executed in a cell-free environment, using only the endogenous housekeeping transcription machinery composed of the core RNA polymerase and sigma factor 70, present in the cytoplasmic extract. This platform is used to construct biochemical systems from DNA programs with the minimal cell as ultimate goal.

Large fluctuations in gene expression are observed at the level of a single gene among the same population of liposomes. However, a more systematic study and chemical optimization will be necessary to determine reproducibility, as well as any source of variability in the molecular components' encapsulation. In particular, centrifugation and transfer of the emulsion into the feeding solution

could be an important process influencing that entrapment. Our preliminary studies suggest that the heterogeneity of the encapsulation of the DNA template is responsible for such variations. Such fluctuations have been already reported and also modeled in liposomes [29, 22]. With our method, we show that increasing the concentration of plasmid can significantly reduce these variations on gene expression inside liposomes.

Acknowledgments

This research was supported by the Defense Advanced Research Projects Agency (DARPA/MTO) Living Foundries program, contract number HR0011-12-C-0065. The authors declare no competing financial interest.

References

1. Auerbach, J. E., & Bongard, J. C. (2014). Environmental influence on the evolution of morphological complexity in machines. *PLoS Computational Biology*, *10*, e1003399.
2. Bedau, M. A. (2003). Artificial life: Organization, adaptation and complexity from the bottom up. *Trends in Cognitive Science*, *7*, 505–512.
3. Calhoun, K. A., & Swartz, J. R. (2005). Energizing cell-free protein synthesis with glucose metabolism. *Biotechnology and Bioengineering*, *90*, 606–613.
4. Caschera, F., & Noireaux, V. (2014). A cost-effective polyposphate-based metabolism fuels an all *E. coli* cell-free expression system. *Metabolic Engineering*, *27*, 29–37.
5. Caschera, F., & Noireaux, V. (2014). Integration of biological parts toward the synthesis of a minimal cell. *Current Opinion in Chemical Biology*, *22*, 85–91.
6. Caschera, F., & Noireaux, V. (2014). A novel *in vitro* metabolic scheme for the construction of a minimal biological cell. In H. Sayama, J. Rieffel, S. Risi, R. Doursat, & H. Lipson (Eds.), *Artificial life 14: Proceedings of the Fourteenth International Conference on the Synthesis and Simulation of Living Systems* (pp. 3–5). Cambridge, MA: MIT Press.
7. Caschera, F., & Noireaux, V. (2013). Synthesis of 2.3 mg/ml of protein with an all *Escherichia coli* cell-free transcription-translation system. *Biochimie*, *99*, 162–168.
8. Caschera, F., Sunami, T., Matsuura, T., Suzuki, H., Hanczyc, M. M., & Yomo, T. (2011). Programmed vesicle fusion triggers gene expression. *Langmuir*, *27*, 13082–13090.
9. Caschera, F., Bedau, M. A., Buchanan, A., Cawse, J., de Lucrezia, D., Gazzola, G., Hanczyc, M. M., & Packard, N. H. (2011). Coping with complexity: Machine learning optimization of cell-free protein synthesis. *Biotechnology and Bioengineering*, *108*, 2218–2228.
10. Caschera, F., Hanczyc, M. M., & Rasmussen, S. (2011). Machine learning for drug design, molecular machines and evolvable artificial cells. In N. Krasnogor (Ed.), *Proceedings of the 13th Annual Conference Companion on Genetic and Evolutionary Computation (GECCO '11)* (pp. 831–832). New York: ACM.
11. Caschera, F., Gazzola, G., Bedau, M. A., Bosch Moreno, C., Buchanan, A., Cawse, J., Packard, N., & Hanczyc, M. M. (2010). Automated discovery of novel drug formulations using predictive iterated high throughput experimentation. *PLoS One*, *5*, e8546.
12. Coyne, C. W., Patel, K., Heureaux, J., Stachowiak, J., Fletcher, D. A., & Liu, A. P. (2014). Lipid bilayer vesicle generation using microfluidic jetting. *Journal of Visualized Experiments*, e51510.
13. Dudley, Q. M., Karim, A. S., & Jewett, M. C. (2015). Cell-free metabolic engineering: Biomanufacturing beyond the cell. *Biotechnology Journal*, *10*(1), 69–82.
14. Fritz, B. R., & Jewett, M. C. (2014). The impact of transcriptional tuning on *in vitro* integrated rRNA transcription and ribosome construction. *Nucleic Acids Research*, *42*, 6774–6785.
15. Fujii, S., Matsuura, T., Sunami, T., Nishikawa, T., Kazuta, Y., & Yomo, T. (2014). Liposome display for *in vitro* selection and evolution of membrane proteins. *Nature Protocols*, *9*, 1578–1591.
16. Griffiths, A. D., & Tawfik, D. S. (2003). Directed evolution of an extremely fast phosphotriesterase by *in vitro* compartmentalization. *The EMBO Journal*, *22*, 24–35.

17. Kuruma, Y., Stano, P., Ueda, T., & Luisi, P. L. (2009). A synthetic biology approach to the construction of membrane proteins in semi-synthetic minimal cells. *Biochimica et Biophysica Acta*, 1788, 567–574.
18. Liu, A. P., & Fletcher, D. A. (2009). Biology under construction: *In vitro* reconstitution of cellular function. *Nature Reviews Molecular Cell Biology*, 10, 644–650.
19. Luisi, P. L., Allegretti, M., Pereira de Souza, T., Steiniger, F., Fahr, A., & Stano, P. (2010). Spontaneous protein crowding in liposomes: A new vista for the origin of cellular metabolism. *ChemBiochem*, 11, 1989–1992.
20. Maeda, Y., Nakadai, T., Shin, J., Uryu, K., Noireaux, V., & Libchaber, A. (2012). Assembly of MreB filaments on vesicular membranes: A synthetic biology approach. *ACS Synthetic Biology*, 1, 53–59.
21. Matsubayashi, H., Kuruma, Y., & Ueda, T. (2014). *In vitro* synthesis of the *E. coli* Sec translocon from DNA. *Angewandte Chemie International Edition in English*, 53, 7535–7538.
22. Nishimura, K., Tsuru, S., Suzuki, H., & Yomo, T. (2015). Stochasticity in gene expression in a cell-sized compartment. *ACS Synthetic Biology*, 4(5), 566–576.
23. Noireaux, V., Maeda, Y. T., & Libchaber, A. (2011). Development of an artificial cell, from self-organization to computation and self-reproduction. *Proceedings of the National Academy of Sciences of the U.S.A.*, 108, 3473–3480.
24. Noireaux, V., & Libchaber, A. (2004). A vesicle bioreactor as a step toward an artificial cell assembly. *Proceedings of the National Academy of Sciences of the U.S.A.*, 101, 17669–17674.
25. Pereira de Souza, T., Steiniger, F., Stano, P., Fahr, A., & Luisi, P. L. (2011). Spontaneous crowding of ribosomes and proteins inside vesicles: A possible mechanism for the origin of cell metabolism. *ChemBiochem*, 12, 2325–2330.
26. Rasmussen, S., Chen, L., Nilsson, M., & Abe, S. (2003). Bridging nonliving and living matter. *Artificial Life*, 9, 269–316.
27. Rivas, G., Vogel, S. K., & Schwille, P. (2014). Reconstitution of cytoskeletal protein assemblies for large-scale membrane transformation. *Current Opinion in Chemical Biology*, 22, 18–26.
28. Ruiz-Mirazo, K., Pereto, J., & Moreno, A. (2004). A universal definition of life: Autonomy and open-ended evolution. *Origins of Life and Evolution of Biospheres*, 34, 323–346.
29. Saito, H., Kato, Y., Le Berre, M., Yamada, A., Inoue, T., Yosikawa, K., & Baigl, D. (2009). Time-resolved tracking of a minimum gene expression system reconstituted in giant liposomes. *ChemBiochem*, 10, 1640–1643.
30. Shin, J., & Noireaux, V. (2012). An *E. coli* cell-free expression toolbox: Application to synthetic gene circuits and artificial cells. *ACS Synthetic Biology*, 1, 29–41.
31. Shin, J., & Noireaux, V. (2010). Efficient cell-free expression with the endogenous *E. coli* RNA polymerase and sigma factor 70. *Journal of Biological Engineering*, 4, 8.
32. Shiomi, H., Tsuda, S., Suzuki, H., & Yomo, T. (2014). Liposome-based liquid handling platform featuring addition, mixing, and aliquoting of femtoliter volumes. *PLoS One*, 9, e101820.
33. Slanzi, D., & Poli, I. Evolutionary Bayesian network design for high dimensional experiments. *Chemometrics and Intelligent Laboratory Systems*, 135, 172–181.
34. Sokolova, E., Spruijt, E., Hansen, M. M. K., Dubuc, E., Groen, J., Chokkalingam, V., Piruska, A., Heus, H. A., & Huck, W. T. S. (2013). Enhanced transcription rates in membrane-free protocells formed by coacervation of cell lysate. *Proceedings of the National Academy of Sciences of the U.S.A.*, 110, 11692–11697.
35. Sole, R. V. (2009). Evolution and self-assembly of protocells. *International Journal of Biochemistry & Cell Biology*, 41, 274–284.
36. Stano, P., D'Aguzzo, E., Bolz, J., Fahr, A., & Luisi, P. L. (2013). A remarkable self-organization process as the origin of primitive functional cells. *Angewandte Chemie International Edition*, 52, 13397–13400.
37. Sun, Z. Z., Hayes, C. A., Shin, J., Caschera, F., Murray, R. M., & Noireaux, V. (2013). Protocols for implementing an Escherichia coli based TX-TL cell-free expression system for synthetic biology. *Journal of Visualized Experiments*, e50762.
38. Swartz, J. R. (2012). Transforming biochemical engineering with cell-free biology. *AIChE Journal*, 58, 5–13.

39. Uno, K., Sunami, T., Ichihashi, N., Kazuta, Y., Matsuura, T., & Yomo, T. (2014). The evolutionary enhancement of genotype-phenotype linkages in the presence of multiple copies of genetic material. *ChemBiochem*, *15*, 2281–2288.
40. Walde, P., Cosentino, K., Engel, H., & Stano, P. (2010). Giant vesicles: Preparations and applications. *ChemBiochem*, *11*, 848–865.
41. Zhou, H. X., Rivas, G., & Minton, A. P. (2008). Macromolecular crowding and confinement: Biochemical, biophysical, and potential physiological consequences. *Annual Review of Biophysics*, *37*, 375–397.

AUTHOR QUERY

AUTHOR PLEASE ANSWER QUERY

During the preparation of your manuscript, the question listed below arose. Kindly supply the necessary information.

1. Please check if the proposed running head is okay.

END OF QUERY